

# Transition from Paired Quantum Hall to Compressible States at the Half Filling of the Lowest Two Landau Levels

E. H. Rezayi<sup>a</sup> and F. D. M. Haldane<sup>b</sup>

<sup>a</sup>*Department of Physics, California State University, Los Angeles, California 90032*

<sup>b</sup>*Department of Physics, Princeton University, Princeton, New Jersey 08544*

(February 2, 2019)

We consider the lowest two Landau levels at half filling. In the higher Landau level ( $\nu = 5/2$ ), we find a first order phase transition separating a compressible striped phase from a paired quantum Hall state. The critical point is very near the Coulomb potential and the transition can be driven by increasing the width of the electron layer. We find a much weaker transition (either second order or a crossover) from pairing to the composite fermion Fermi liquid behavior. A very similar picture is obtained for the lowest Landau level but the transition point is not near the Coulomb potential.

73.20.Dx, 73.40.Kp, 73.50.Jt

A two dimensional electron gas in an intense perpendicular magnetic field displays a host of collective ground states. The underlying reason is the formation of two-dimensional Landau levels in which the kinetic energy is completely quenched. In the resulting macroscopically degenerate Hilbert space, only the Coulomb potential remains, making the system strongly interacting. The fractional quantum Hall effect [1], at rational fillings of the Landau levels, is a manifestations of such a ground state (GS). At half filling, the electron gas exhibits remarkably diverse behavior in the first three Landau levels. In the lowest Landau level,  $\rho_{xx}$  shows a shallow minimum and no plateau [2] in  $\rho_{xy}$ . This behavior has been associated with a compressible Fermi-liquid-like state [3] of composite fermions [4]. In sharp contrast, a plateau in  $\rho_{xy}$  and activated  $\rho_{xx}$  has been observed at filling factor  $\nu = 5/2$  [5], indicating the formation of an incompressible quantum Hall effect state. Above the second Landau level, for  $\nu = 9/2, 11/2, 13/2$ , the transport becomes highly anisotropic [6–8] which is widely believed to result from a compressible charge density wave-like (CDW) GS [9–11]. Some years ago we proposed [12] a spin-singlet wavefunction for the 5/2 effect based on the idea of pairing [13] electrons. Moore and Read [14] (MR), building on the analogy of this state to BCS pairing of CF's, proposed a spin-polarized pairing wavefunction:

$$\Psi_{\text{HR}}(\{z_i\}) = \prod_{i,j} (z_i - z_j)^2 \text{Pf} \left( \frac{\alpha_i \beta_j - \beta_i \alpha_j}{(z_i - z_j)^2} \right), \quad (1)$$

$$\Psi_{\text{MR}}(\{z_i\}) = \prod_{i,j} (z_i - z_j)^2 \text{Pf} \left( \frac{\alpha_i \alpha_j}{z_i - z_j} \right), \quad (2)$$

where  $\alpha$  and  $\beta$  are spinor coordinates for up and down spins, and  $\text{Pf} A_{i,j}$  is the Pfaffian of the matrix  $A$ . Originally, the spatial part of Eq. 1 was given as the Jastrow factor and the determinant of the inverse distances squared.

There have been suggestions that the 5/2 state may be polarized [15] and the MR wavefunction may be a

possible candidate [16] for it. In this paper we present numerical evidence which suggests that the  $\nu = 5/2$  effect indeed derives from a paired state which is closely related to the MR polarized state or, more precisely, to the state obtained by particle-hole (PH) symmetrization of the MR state. Further we show why the transport may not be quantized [17] and may become anisotropic upon tilting the field, as observed [18,19]. We find a first-order phase transition from a striped phase to a paired state, followed by another transition to a Fermi-liquid state, which is either second order or a continuous crossover. Our conclusions are based on numerical studies for up to 16 electrons in two geometries: sphere and torus. The torus is particularly convenient for investigating the nature of the ground state at  $\nu = 1/2$ . All three states of interest— composite fermion Fermi surface, pairing and CDW— are realized at flux  $N_\phi = 2N$  (in units of flux quanta). On the other hand this is not the case on the sphere, where they all occur at different flux values for the same number of electrons introducing unwanted finite-size effects. We only consider states within a given Landau level and hence discard the (constant) kinetic energy. The Hamiltonian is:

$$H = \sum_{m=0}^{\infty} \sum_{i<j} \sum_{\mathbf{q}} e^{-q^2/2} L_m(q^2) V_m e^{i\mathbf{q}\cdot(\mathbf{R}_i - \mathbf{R}_j)}, \quad (3)$$

where  $\mathbf{R}_i$  is the guiding center [20] coordinate of the  $i$ th electron,  $L_m(x)$  are the Laguerre polynomials, and  $V_m$  is the energy of a pair of electrons in a state of relative angular momentum  $m$ . These are the pseudo-potential parameters [20,21]. The magnetic length is set to 1. Unless otherwise specified the data presented here is for ten fully polarized electrons in a hexagonal unit cell (UC).

The Fermi-liquid state is well described by a Fermi sea of composite fermions [22,23], which on the torus is [23]:

$$\Psi_{CF} = \det_{i,j} \exp(i\mathbf{K}_i \cdot \mathbf{R}_j) \Psi_B(z_1, z_2, \dots, z_N), \quad (4)$$

where  $\Psi_B$  is the Laughlin wavefunction for bosons at  $\nu = 1/2$ ; the  $\{\mathbf{K}_i\}$  are distinct (and belong to the usual

set allowed by the PBC's), and are clustered together to form a filled "Fermi Sea" centered on  $\mathbf{K}_{av} = \sum \mathbf{K}_i/N$ . The CF state is invariant under uniform shift in k-space by an allowed  $\mathbf{K}$  vector. There are  $N^2$  distinct values of total momentum quantum numbers (Bloch vectors)  $N\mathbf{K}_{av}$  as  $\mathbf{K}_{av}$  is only meaningful relative to the lattice of allowed  $\mathbf{K}$ 's. There are 4 distinct values of  $\mathbf{K}_{av}$  which are invariant under rotation by  $\pi$ : 1)  $\mathbf{K}_{av}=0$  and 2)  $\mathbf{K}_{av}$  halfway between allowed  $\mathbf{K}$ -vectors (3 distinct values which are the 3 distinct values of  $\mathbf{k}$  for the MR state on the torus).

The CF state is essentially particle hole symmetric (99.935%) and obtains large overlaps (99.25%) with the exact GS of the Coulomb potential in the lowest Landau level. This is remarkably large given that the symmetry reduced Hilbert space has a dimension of about 1000. There is no known Hamiltonian to produce the above wavefunction as an eigenstate. We therefore evaluate Eq. 4 directly. As stated above, On the torus the periodic MR state [16] is 3-fold degenerate (excluding CM degeneracy), and can be obtained as the zero energy ground state of the 3-body short range potential [16]:

$$H = - \sum_{i < j < k} \mathcal{S}_{i,j,k} \{ \nabla_i^4 \nabla_j^2 + \nabla_i^2 \nabla_j^4 \} \delta^2(\mathbf{r}_i - \mathbf{r}_j) \delta^2(\mathbf{r}_j - \mathbf{r}_k),$$

where  $\mathcal{S}_{i,j,k}$  is the symmetrization operator in  $i, j$  and  $k$ . It is important to note that the 3-body H explicitly breaks PH symmetry and the MR state does not possess definite parity under PH transformations. For the ten electron system with hexagonal UC it is 77% PH symmetric. In contrast, two-body potentials are PH invariant and eigenstates have a definite PH parity [24]. For these

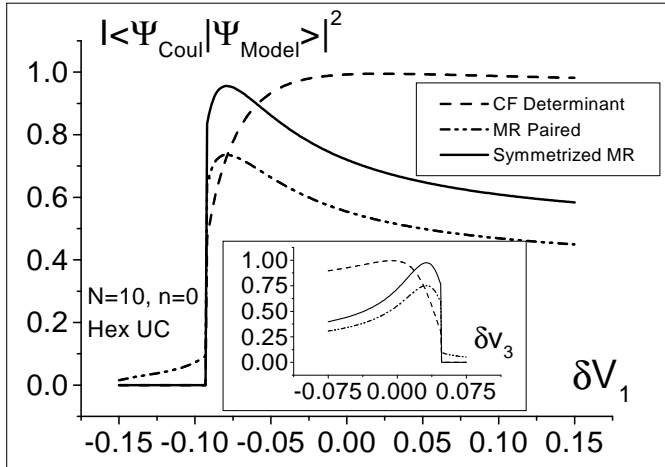


FIG. 1. The overlap squared of the exact wavefunction with both the CF determinant state and the MR pairing state as only the short-range component ( $V_1$ ) of the Coulomb potential in  $n = 0$  Landau level is varied. The inset gives same but when  $V_3$  is varied. the MR state as well as the other two have wave vectors  $\mathbf{k} = (0, 3.011)$ , and  $(2.608, \pm 1.506)$ .

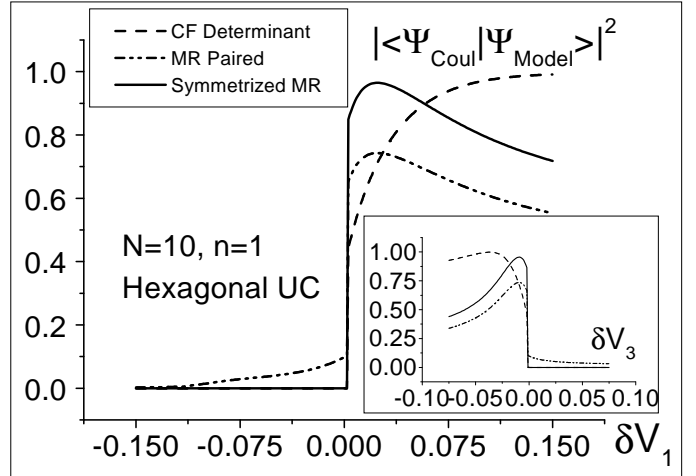


FIG. 2. Same as Fig. 1 but for the  $n = 1$  Landau level.

potentials, we find the nature of the ground state depends on the relative strengths of various pseudo-potential parameters, in particular the first two  $V_1$  and  $V_3$  (even  $m$  pseudo-potentials do not affect polarized states). Figs. 1, 2 and 3 show the overlaps of both of the above model states with the exact one in the two lowest Landau levels as  $V_1$  in the Coulomb potential is varied. Varying  $V_3$  alone (the insets) or varying both  $V_1$  and  $V_3$  yield a very similar picture, although they act in opposite directions.

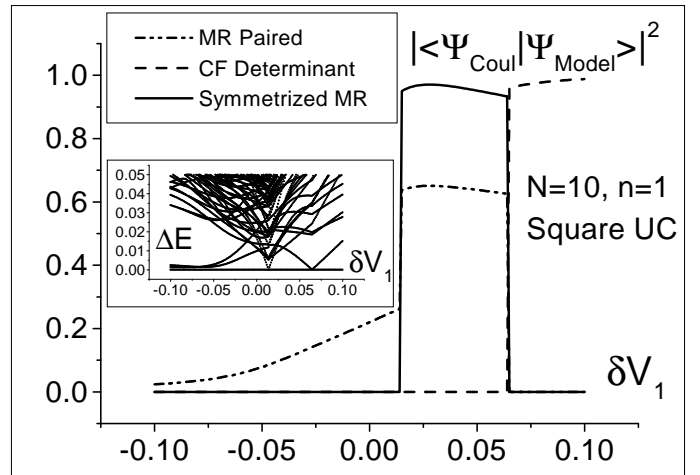


FIG. 3. Same as Fig. 2 but for a square unit cell. The inset shows the excitation spectrum (the GS energy is subtracted) as a function of  $\delta V_1$ . The transition points are marked by the collapse of the gap. In the striped phase (left portion) one recovers the typical degeneracies seen in the  $n = 2, 3$  LL's.

A first-order phase transition from a compressible state to the pairing state is seen clearly. The transition is very close to the Coulomb value (zero of the horizontal axis) for the excited Landau level and is farther to the left for the lowest Landau level. Later, we will present evidence

that the compressible state is like the stripe-phase state seen in the higher ( $n \geq 2$ ) Landau levels.

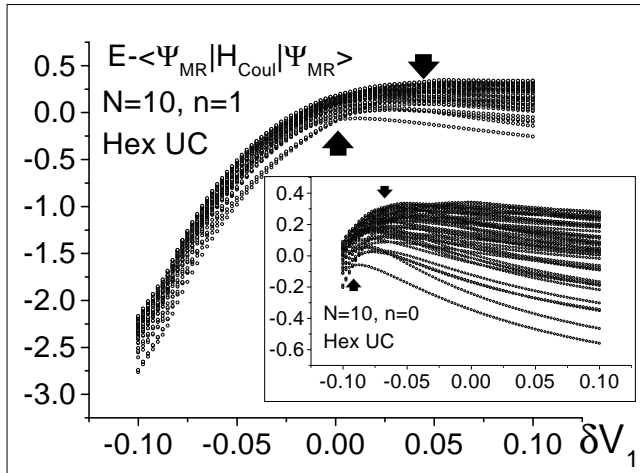


FIG. 4. The low lying spectrum (relative to the variational energy of the MR state) plotted vs.  $\delta V_1$  for the  $n = 1$  LL. The Coulomb point is  $\delta V_1 = 0$ . The inset shows the same but for the lowest LL. The energies are scaled by the bandwidth of the two-particle system. The region between the arrows is the strong pairing regime.

The surprising feature in these pictures is the absence of an additional transition from the paired state to the compressible Fermi-liquid state of composite fermions as  $V_1$  is increased further. The same feature is seen in the excitation spectrum. Fig. 4 shows the low lying excitation spectrum (first fifty energy levels) as a function of  $V_1$ . Again, there is only one first-order level crossing transition (shown by up arrows). The crossing levels have the same translational and rotation by  $\pi$  symmetry but belong to opposite parities under PH transformation. The MR state having mixed symmetry has a finite overlap with the exact GS on both sides of the transition. Past this point the excitation spectrum of the system ( $E$  vs.  $k$ , not shown) gradually evolves from gapped paired to the compressible CF Fermi-liquid-like spectrum [22,23]. This same type of crossover behavior is also seen on the sphere and the more generic geometries on the torus. In the latter cases, the Fermi surface state has the same wave vector  $\mathbf{k}$  as one of the three MR states whenever the Fermi surface is *symmetric* under rotations by  $\pi$ . The crossover is approximately at the point where the spectrum begins to change which occurs at the level crossings of the *excited* states (shown by down arrows).

The hallmark of a compressible state is the sensitivity of its  $\mathbf{k}$  to the geometry of the UC. For example, the Fermi surface for 10 electrons in a square UC does not have rotation by  $\pi$  symmetry and its  $\mathbf{k}$  is different from the MR state. A sharp transition is seen in this case (Fig. 3). The picture suggested by our studies is that the system may always be paired and interpolates smoothly be-

tween strong and weak pairing regimes as the interaction potential is varied. In the weak pairing regime such a system will exhibit CF Fermi-liquid-like behavior at energy scales above the gap but paired quantum Hall behavior at lower energies. A first order transition between the pairing and CF Fermi-liquid states is not supported by our studies. However, in the thermodynamic limit a second order phase transition between these states cannot be ruled out and remains an alternate possibility.

In agreement with the above, we have also found a substantial pairing character for the Coulomb potential in the lowest Landau level, even though we are far away from the strong pairing regime and the GS is completely dominated by the CF Fermi liquid wavefunction. In fact, the weight of the paired state in the exact ground state of the pure Coulomb potential increases with system size: in the spherical geometry for  $N = 12, 14$  and  $16$  ( $N_\phi = 2N - 3$ ) we find these weights to be 43%, 52% and 56%, despite the fact that the relevant ( $L = 0$ ) Hilbert space grows twenty fold. This is consistent with having weakly bound pairs with sizes larger than the system size.

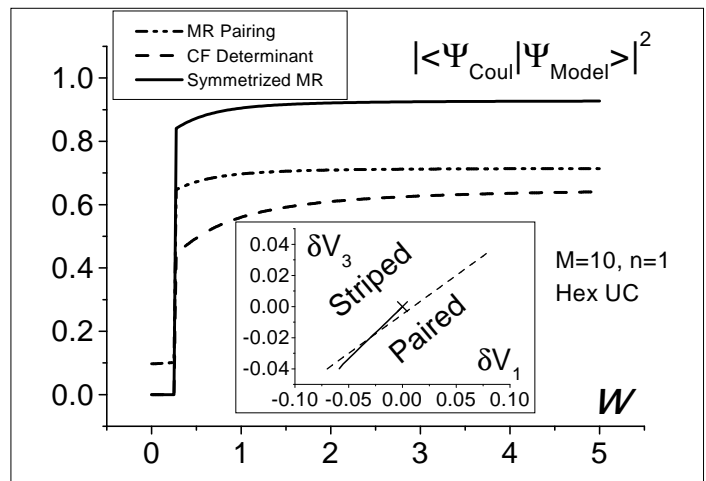


FIG. 5. The overlap squared of the two model states as the layer width  $w$  is varied in the  $n = 1$  Landau level. The inset shows the boundary between striped and paired phases and how layer thickness changes  $\delta V_1$  and  $\delta V_3$  as  $w$  is varied from 0 (at the cross) to 1. The system crosses the phase boundary at  $w = 0.3$  along the solid line.

It is interesting to note that both the overlaps and the low lying spectrum for the  $n = 0$  and the  $n = 1$  Landau levels as a function of  $\delta V_1$  are very similar. The pairing regime is somewhat broader and is shifted to the right for the  $n = 1$  Landau level, bringing it very near the pure Coulomb value. We believe that the proximity of the Coulomb potential to the critical point is the principal reason behind the disappearance of the paired Hall state upon tilting the field. We have found that varying the width of the 2-D layer drives this transition in several different geometries that we studied. The criti-

cal width varied from 0.23 to 2.4 in these systems. We have not yet investigated tilted field effects but believe it will have a similar effect to layer width in driving the transition. Fig. 5 shows the overlap (squared) as a function of the layer width in the  $n = 1$  Landau level. We have used the Fang-Howard model for layer profile (with  $w = 2b$ ) [20,25]. In the lowest Landau level, the GS of the Coulomb potential is well in the CF sea regime. Increasing the layer width improves the pairing correlations continuously with weights reaching 64% (from 54% for the thin layer) for very thick layers. However this becomes quite large (about 83%) once the PH symmetric part of MR wavefunction is kept. For both Landau levels, increasing layer width increases the pairing correlations which is also seen in Monte-Carlo calculations [26].

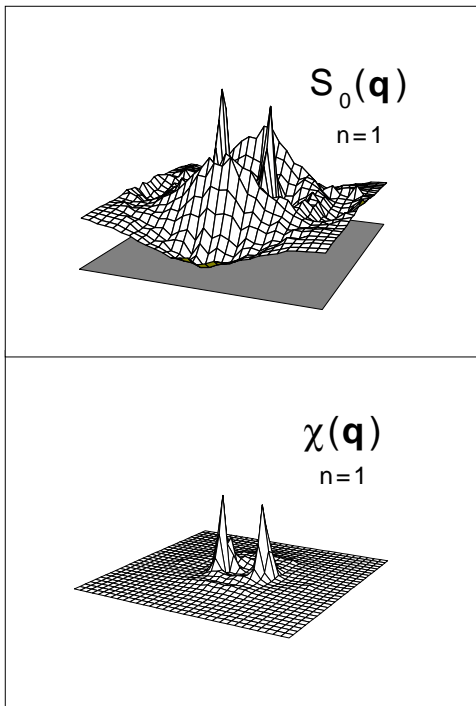


FIG. 6. three-dimensional plot of the static structure factor  $S_0(\mathbf{q})$  and charge susceptibility  $\chi(\mathbf{q})$  as a function of the  $\mathbf{q}$ . The maximum height in  $\chi$  is 1229.2 compared to 20-50 for incompressible states.

We next turn to the compressible state seen before the transition. To investigate its nature we have calculated both the guiding center structure factor  $S_0(\mathbf{q})$  and the density response susceptibility  $\chi(\mathbf{q})$ . Fig. 6 shows a 3-dimensional plot that has combined results from several geometries for ten electrons. The strongest response was at hexagonal geometry which, interestingly, was *uniaxial* at wave vectors  $\mathbf{q}^* = (0, \pm 1.2)$ . The response at other wave vectors with six-fold symmetry was smaller by a factor of 50 or less. Similarly, for rectangular geometries with different aspect ratios, the response was much weaker than the  $n \geq 2$  [11] ground states. However, this

is possibly a finite-size effect. As seen in the inset of Fig. 3 the degeneracies that give rise to a strong response [11] are not well developed in the finite-size system until  $V_1$  is lowered by 0.05 from its Coulomb value.

An interesting question is whether in the lowest Landau level the crossover to the paired state can be driven by layer thickness or other external conditions such as front and back gate controls in the experiments. Our study suggests that for this to happen,  $V_1$  needs to be weakened by 15%-20% of its Coulomb value relative to the other pseudo-potentials. However, the overlaps (squared) did not increase beyond 64% even for very thick layers and the GS remained CF Fermi-liquid in character. The needed reduction of  $V_1$  may be too large for 2-D electrons in Ga-As. However, it may prove to be easier in a 2-D hole system [8]. In this case, the untilted  $\nu = 5/2$  state is in the compressible regime and shows anisotropic transport. This in turn may mean that, for  $\nu = 1/2$  the system is nearer to the strong pairing regime.

We acknowledge useful discussions with R. Morf, J. Eisenstein, and especially N. Read. Supported by NSF DMR-9420560 (EHR) and DMR-9809483 (FDMH). We thank ITP-UCSB for their hospitality during the ‘‘Disorder and Interaction in Quantum Hall and Mesoscopic Systems’’ workshop supported by NSF-PHY94-07194.

- 
- [1] For reviews, see, *e. g. The Quantum Hall Effect*, 2nd Ed., edited by R. E. Prange and S. M. Girvin (Springer, New York, 1990); *Perspectives in Quantum Hall Effect*, edited by S. Das Sarma and A. Pinczuk (Wiley, New York, 1997).
  - [2] R.L. Willett, M.A. Paalanen, K.W. West, L.N. Pfeiffer, and D.J. Bishop, *Phys. Rev. Lett.* **65**, 112 (1990).
  - [3] B. I. Halperin, P. A. Lee, and N. Read, *Phys. Rev. B* **47**, 7312 (1993).
  - [4] J.K. Jain, *Phys. Rev. Lett.* **63**, 199 (1989).
  - [5] R. Willett, J.P. Eisenstein, H.L. Störmer, D.C. Tsui, A.C. Gossard, and J.H. English, *Phys. Rev. Lett.* **59**, 1776 (1987).
  - [6] M. P. Lilly, K. B. Cooper, J. P. Eisenstein, L. N. Pfeiffer, and K. W. West, *Phys. Rev. Lett.* **82**, 394 (1999).
  - [7] R. R. Du, D. C. Tsui, H. L. Störmer, L. N. Pfeiffer, K. W. Baldwin, and K. W. West, *Solid State Commun.* **109**, 389 (1999).
  - [8] M. Shayegan and H.C. Manoharan, cond-mat/9903405.
  - [9] A. A. Koulakov, M. M. Fogler, and B. I. Shklovskii, *Phys. Rev. Lett.* **76**, 499 (1996); *Phys. Rev. B* **54**, 1853 (1996).
  - [10] R. Moessner and J. T. Chalker, *Phys. Rev. B* **54**, 5006 (1996).
  - [11] E.H. Rezayi, F.D.M. Haldane and Kun Yang, cond-mat/9903258.
  - [12] F.D.M. Haldane and E. H. Rezayi, *Phys. Rev. Lett.* **60**, 956 (1988); *Phys. Rev. Lett.* **60**, E1886 (1988).

- [13] B.I. Halperin, *Helv. Phys. Acta*, **56**, 75 (1983).
- [14] G. Moore and N. Read, *Nucl. Phys. B***360**, 362 (1991).
- [15] R.H. Morf, *Phys. Rev. Lett.* **80**, 1505 (1998)
- [16] M. Greiter, X.-G. Wen and F. Wilczek, *Phys. Rev. Lett.* **66**, 3205 (1991); *Nucl. Phys. B* **374**, 567 (1992).
- [17] J.P. Eisenstein, R.L. Willett, H.L. Störmer, D.C. Tsui, A.C. Gossard and J.H. English, *Phys. Rev. Lett.* **61**, 997 (1988).
- [18] W. Pan, R.R. Du, H.L. Störmer, D.C. Tsui, L.N. Pfeiffer, K.W. Baldwin and K.W. West, *cond-mat/9903160*.
- [19] M.P. Lilly, K.B. Cooper, J.P. Eisenstein, L.N. Pfeiffer and K.W. West, *cond-mat/9903196*
- [20] F. D. M. Haldane, in *The Quantum Hall Effect*, Ref. [1].
- [21] For the Coulomb potential in  $n = 0$  LL these are  $V_m^0 = \Gamma(m + 1/2)/(2\Gamma(m + 1))$ , and for  $n = 1$  they are  $V_m^1 = (m - 3/8)(m - 11/8)\Gamma(m - 3/2)/(2\Gamma(m + 1))$ .
- [22] E. Rezayi and N. Read, *Phys. Rev. Lett.* **72**, 900 (1994).
- [23] F. D. M. Haldane *et al.*, unpublished.
- [24] This is true for reflection symmetric PBC's.
- [25] R. E. Prange, in *The Quantum Hall Effect*, Ref. [1].
- [26] K. Park, V. Melik-Alaverdian, N.E. Bonesteel and J.K. Jain, *Phys. Rev. B* **58**, 10167 (1998).